Available online at www.eccomasproceedia.org
Eccomas Proceedia COMPDYN (2017) 1304-1311

ECCOMAS
Proceedia

COMPDYN 2017
6th ECCOMAS Thematic Conference on
Computational Methods in Structural Dynamics and Earthquake Engineering
M. Papadrakakis, M. Fragiadakis (eds.)
Rhodes Island, Greece, 15–17 June, 2017

INVERSE MASS MATRIX VIA THE METHOD OF LOCALIZED LAGRANGE MULTIPLIERS

José A. González[1], R. Kolman[2], S.S. Cho[3], C. A. Felippa[4], K.C. Park[4]

[1]Escuela Técnica Superior de Ingeniería, Universidad de Sevilla
Camino de los Descubrimientos s/n, Seville E-41092, Spain
e-mail: japerez@us.es

[2]Institute of Thermomechanics, The Czech Academy of Sciences
Dolejškova 5, 182 00 Prague, Czech Republic
e-mail: kolman@it.cas.cz

[3]Reactor Mechanical Engineering Division, Korea Atomic Energy Research Institute
999-111 Daedeok-Daero, Yuseong-gu, Daejeon 305-353, Republic of Korea
e-mail: sscho96@kaeri.re.kr

[4]Department of Aerospace Engineering Sciences
University of Colorado at Boulder, CO 80309-429, USA
e-mail: {carlos.felippa,kcpark}@colorado.edu

Keywords: Inverse mass matrix, explicit time integration, localized Lagrange multipliers; partitioned analysis.

Abstract. *An efficient method for generating the mass matrix inverse is presented, which can be tailored to improve the accuracy of target frequency ranges and/or wave contents. The present method bypasses the use of biorthogonal construction of a kernel inverse mass matrix that requires special procedures for boundary conditions and free edges or surfaces, and constructs the free-free inverse mass matrix employing the standard FEM procedure. The various boundary conditions are realized by the the method of localized Lagrange multipliers. Numerical experiments with the proposed inverse mass matrix method are carried out to validate the effectiveness proposed technique when applied to vibration analysis of bars and beams. A perfect agreement is found between the exact inverse of the mass matrix and its direct inverse computed through biorthogonal basis functions.*

doi: 10.7712/120117.5493.17792

1 INTRODUCTION

Recently, Tkachuk and Bischoff [1] presented an innovative method for constructing an inverse mass matrix based on Hamilton's principle with $(\mathbf{p}, \mathbf{u})$-variables. A key idea in their work is the discretization of the momentum-based kinetic energy in terms of a set of biorthogonal basis functions corresponding to the displacement basis functions. The method proposed in [1] resorts to non-standard finite element construction with special tailoring for treating the Dirichlet boundary terms. Hence, considerable modifications of the existing finite element software modules are required. When one contemplates element-by-element construction of the inverse of the global mass matrix, many degrees of freedom belong to the cross points and boundary nodes, which implies that one has to replace the existing mass matrix routines by specially constructed mass matrix inverse.

The present method, while employing the same momentum-velocity formulation as adopted in [1] only as a formulation vehicle, utilizes standard FEM procedures, thus alleviates the special treatments associated the use of biorthogonal construction and mass matrix modification via a penalty procedure.

2 BASIS FOR CONSTRUCTING INVERSE MASS MATRIX VIA THE LOCALIZED LAGRANGE MULTIPLIERS

The prevailing practice for computing the mass matrix $\mathbf{M}$ in the finite element method is to use a bilinear form of the system kinetic energy T, viz.,

$$T = \int_{\Omega} \tfrac{1}{2}\rho \boldsymbol{v}(\mathbf{x}, t) \cdot \boldsymbol{v}(\mathbf{x}, t)\, d\Omega \approx \tfrac{1}{2}\dot{\mathbf{u}}(t)^{\mathsf{T}}\mathbf{M}\,\dot{\mathbf{u}}(t) \tag{1}$$

where $\boldsymbol{v}(\mathbf{x}, t)$ and $\dot{\mathbf{u}}(t)$ are the continuum velocity and discrete approximate velocity, respectively. Since our objective is to generate the inverse mass matrix directly, instead of employing matrix inversion, we employ a dual form of the kinetic energy:

$$T = \int_{\Omega} \frac{1}{2\rho}\boldsymbol{p}(\mathbf{x}, t) \cdot \boldsymbol{p}(\mathbf{x}, t)\, d\Omega \approx \tfrac{1}{2}\mathbf{p}(t)^{\mathsf{T}}\mathbf{C}\mathbf{p}(t) \tag{2}$$

where $\boldsymbol{p}(\mathbf{x}, t)$ and $\mathbf{p}(t)$ are respectively the continuum and discrete approximate momentum vectors, and $\mathbf{C}$ is defined as the Reciprocal Mass Matrix (RMM).

It will be shown that an inverse of the mass matrix can be obtained via:

$$\mathbf{M}^{-1} = \mathbf{A}^{-\mathsf{T}}\mathbf{C}\mathbf{A}^{-1} \tag{3}$$

where $\mathbf{A}$ is the dual-base projection matrix, that can be transformed into a diagonal area/volume-like matrix. Hence, the computational simplicity of obtaining an inverse of the mass-matrix via this new route.

To this end, we invoke Hamilton's principle for constrained elastodynamic problems. This principle states that *the path followed by a dynamic system is the one which minimizes the action integral of the Lagrangian*; condition that can be expressed using the following three-field variational form:

$$\delta H(\boldsymbol{u}, \boldsymbol{p}, \boldsymbol{\ell}) = \int_{t_1}^{t_2} \delta\left\{T(\dot{\boldsymbol{u}}, \boldsymbol{p}) - U(\boldsymbol{u}, \boldsymbol{\ell}) + W(\boldsymbol{u})\right\}\, dt = 0 \tag{4}$$

were δT is the virtual kinetic energy, δU the virtual elastic energy and δW the virtual work done by the external loads, magnitudes that can be expressed:

$$\delta T = \int_\Omega \delta(\tfrac{1}{2}\boldsymbol{p}\cdot\dot{\boldsymbol{u}})\,d\Omega \tag{5}$$

$$\delta U = \int_\Omega \delta\boldsymbol{\varepsilon} : \boldsymbol{\sigma}\,d\Omega + \int_\Gamma \delta\left\{\boldsymbol{\ell}\cdot(\boldsymbol{u}-\boldsymbol{u}_b)\right\}\,d\Gamma \tag{6}$$

$$\delta W = \int_\Omega \delta\boldsymbol{u}\cdot\boldsymbol{f}\,d\Omega \tag{7}$$

with known displacement boundary conditions $\boldsymbol{u}_b$ imposed at interface Γ by using a field of localized Lagrange multipliers $\boldsymbol{\ell}$ and external body forces per unit volume $\boldsymbol{f}$ acting on Ω.

By making use of the momentum-velocity relation ($\boldsymbol{p}=\rho\dot{\boldsymbol{u}}$) in the following identity:

$$\tfrac{1}{2}\boldsymbol{p}\cdot\dot{\boldsymbol{u}} = \boldsymbol{p}\cdot\dot{\boldsymbol{u}} - \frac{1}{2\rho}\boldsymbol{p}\cdot\boldsymbol{p} \tag{8}$$

we can obtain an equivalent expression for the virtual kinetic energy per unit volume:

$$\delta\left(\tfrac{1}{2}\boldsymbol{p}\cdot\dot{\boldsymbol{u}}\right) = \delta\dot{\boldsymbol{u}}\cdot\boldsymbol{p} + \delta\boldsymbol{p}\cdot\left(\dot{\boldsymbol{u}} - \frac{1}{\rho}\boldsymbol{p}\right) \tag{9}$$

and finally performing an integration by parts of the second term of the last equation yields:

$$\int_{t_1}^{t_2} \delta\dot{\mathbf{u}}\cdot\boldsymbol{p}\,dt = -\int_{t_1}^{t_2}\delta\boldsymbol{u}\cdot\dot{\boldsymbol{p}}\,dt \tag{10}$$

relation that can be used to eliminate the virtual velocity field from the formulation.

Introducing previous identities, (9) and (10), into the principle of stationary action (4), we obtain the final the three-field variational form of the Hamilton's principle for constrained elastodynamics:

$$\delta H(\boldsymbol{u},\boldsymbol{p},\boldsymbol{\ell}) = \int_{t_1}^{t_2}\left\{\int_\Omega \delta\boldsymbol{p}\cdot\left(\dot{\boldsymbol{u}}-\frac{1}{\rho}\boldsymbol{p}\right)\,d\Omega - \int_\Omega\left(\delta\boldsymbol{u}\cdot\dot{\boldsymbol{p}}+\delta\boldsymbol{\varepsilon}:\boldsymbol{\sigma}\right)\,d\Omega + \int_\Omega\delta\boldsymbol{u}\cdot\boldsymbol{f}\,d\Omega \right.$$
$$\left. -\int_\Gamma \delta\boldsymbol{u}\cdot\boldsymbol{\ell}\,d\Gamma - \int_\Gamma\delta\boldsymbol{\ell}\cdot(\boldsymbol{u}-\boldsymbol{u}_b)\,d\Gamma\right\}\,dt = 0 \tag{11}$$

expression that will be used to derive the equations of motion.

Discretization in space of this mixed form is performed by using independent shape functions for displacements, momenta and Lagrangian multipliers. We carry out then a standard mixed FEM discretization with independent shape functions for the three fields:

$$\boldsymbol{u} = \mathbf{N}_u\mathbf{u}, \qquad \boldsymbol{p} = \mathbf{N}_p\mathbf{p}, \qquad \boldsymbol{\ell} = \mathbf{N}_\lambda\boldsymbol{\lambda} \tag{12}$$

and introducing these approximations in (11) one obtains the following set of semi-discrete equations:

$$\mathbf{A}^\mathsf{T}\dot{\mathbf{u}} - \mathbf{C}\mathbf{p} = \mathbf{0} \qquad \textit{Momentum equation} \tag{13}$$

$$\mathbf{A}\dot{\mathbf{p}} + \mathbf{B}\boldsymbol{\lambda} = \mathbf{r} \qquad \textit{Equilibrium equation} \tag{14}$$

$$\mathbf{B}^\mathsf{T}\mathbf{u} - \mathbf{L}_b\mathbf{u}_b = \mathbf{0} \qquad \textit{Boundary (and interface) constraints} \tag{15}$$

$$-\mathbf{L}_b^\mathsf{T}\boldsymbol{\lambda} = \mathbf{0} \qquad \textit{Newton's 3rd law on the boundaries} \tag{16}$$

where vector $\mathbf{r} = \mathbf{f} - \mathbf{f}^{int}$ is the external-internal forces residual, the internal forces for linear problems are simply given by $\mathbf{f}^{int} = \mathbf{Ku}$ and the matrix components are expressed:

$$\mathbf{A} = \int_{\Omega} \mathbf{N}_u^{\mathsf{T}} \, \mathbf{N}_p \, d\Omega \tag{17}$$

$$\mathbf{C} = \int_{\Omega} \frac{1}{\rho} \mathbf{N}_p^{\mathsf{T}} \, \mathbf{N}_p \, d\Omega \tag{18}$$

$$\mathbf{B} = \int_{\Gamma} \mathbf{N}_u^{\mathsf{T}} \, \mathbf{N}_\lambda \, d\Gamma \tag{19}$$

$$\mathbf{L}_b = \int_{\Gamma} \mathbf{N}_\lambda^{\mathsf{T}} \, \mathbf{N}_{ub} \, d\Gamma \tag{20}$$

where $\mathbf{A}$ is the global projection matrix, $\mathbf{C}$ the global reciprocal mass matrix, $\mathbf{B}$ the boundary assembly operator and $\mathbf{L}_b$ is the Localized multipliers assembly matrix.

Eliminating symbolically the momentum variable ($\mathbf{p}$) from (13) and (14), one obtains the classical equation of motion expressed in terms of displacements:

$$\left(\mathbf{A}\mathbf{C}^{-1}\mathbf{A}^{\mathsf{T}}\right) \ddot{\mathbf{u}} + \mathbf{B}\boldsymbol{\lambda} = \mathbf{r} \tag{21}$$

with the mass matrix approximated as:

$$\mathbf{M} = \mathbf{A}\mathbf{C}^{-1}\mathbf{A}^{\mathsf{T}} \tag{22}$$

and observe that there must exist an inverse mass matrix (denoted as $\mathbf{M}^{-1}$) given by:

$$\mathbf{M}^{-1} = \mathbf{A}^{-\mathsf{T}}\mathbf{C}\mathbf{A}^{-1} \tag{23}$$

assuming that the global projection matrix is invertible.

Since the objective of the present work is to obtain inverse mass-matrices in efficient and accurate ways, one must insist on easily to invert *diagonal* or narrowly banded projection matrices. This can be accomplished by diagonalizing the projection $\mathbf{A}$-matrix given in (17), leaving the task of constructing the reciprocal $\mathbf{C}$-matrix efficiently and accurately.

3 CONSTRUCTION OF THE MASS INVERSE

For the calculation of the inverse mass-matrix, biorthogonal basis functions must be first build for each particular finite element. However, basis functions are known for a limited number of elements, such as line, triangular, quadrilateral and tetrahedral elements. Therefore, we propose a different route for the evaluation of the mass-matrix inverse that bypasses this necessity through the following steps:

1. Consider all the structures as free-floating.
2. Approximate the element projection matrix $\mathbf{A}_e$ by a lumping of the element mass-matrix.
3. Compute the element reciprocal mass-matrix $\mathbf{C}_e$ from a direct inversion of the element mass-matrix.
4. Assemble the global projection and reciprocal matrices and compute the global mass-matrix inverse.

5. Impose boundary conditions using localized Lagrange multipliers[2]-[3].

The first four steps of this process are described next and the last step, that is a little bit more involved, will be analyzed in the next Section.

First, we consider an element at a time by utilizing the element mass matrices existing in standard FEM software systems. Second, we use the element mass-matrix to approximate the element projection matrix by diagonalization, viz.:

$$[\mathbf{A}_e]_{ii} = \frac{1}{\rho_e} \sum_j [\mathbf{M}_e]_{ij} \tag{24}$$

assuming that the density is constant inside the element. Third, the elemental reciprocal mass-matrix is evaluated inverting numerically the element mass-matrix:

$$\mathbf{C}_e = \mathbf{A}_e^{\mathsf{T}} \mathbf{M}_e^{-1} \mathbf{A}_e \tag{25}$$

where $(\mathbf{A}_e, \mathbf{C}_e, \mathbf{M}_e)$ are elemental matrices, and particularly $\mathbf{A}_e$ is a diagonalized matrix.

Finally, we proceed with the assembly of the global reciprocal mass-matrix:

$$\mathbf{C} = \mathop{\mathsf{A}}_{e=1}^{n_e} \mathbf{C}_e \tag{26}$$

and the global projection matrix:

$$\mathbf{A} = \mathop{\mathsf{A}}_{e=1}^{n_e} \mathbf{A}_e \tag{27}$$

observing that as long as the elemental $\mathbf{A}_e$ is diagonal, so is the assembled matrix $\mathbf{A}$ and its inverse. These steps permit to evaluate the inverse of the global mass-matrix through expression (23) in an efficient way.

4 NUMERICAL RESULTS

We have assessed the performance of the present mass-matrix inverse for bar and beam structural elements, in both free-free states and cantilevered conditions. In so doing, for the derivation of elemental reciprocal mass-matrix $\mathbf{C}_e$, we have utilized a parametrized elemental mass-matrix expressed in the form:

$$\mathbf{M}_e = (1-\beta)\mathbf{M}_e^c + \beta \mathbf{M}_e^l \tag{28}$$

in which a parameter $\beta \in [0, 1]$ is used to balance between the consistent element mass-matrix $\mathbf{M}_e^c$ and the lumped element mass-matrix $\mathbf{M}_e^l$. Using $\beta = \{0, 0.5, 1\}$ the element mass-matrix is then easily reduced respectively to the consistent mass-matrix (CMM), averaged mass-matrix (AMM) and lumped mass-matrix (LMM). Unless otherwise stated, in the following numerical experiments we employ AMM as a reference and compute the mass-matrix inverse using RMM with $\beta = 0.5$ to test the proposed methodology.

4.1 Frequencies of a free-free and a fixed-free bar

In this first example, we consider a long bar of length $L = 1m$ with a rectangular section of width $b = 0.05$ m and thickness $h = 0.01$ m. The material of the bar is linear elastic, with Young's modulus $E = 69$ GPa and a constant density $\rho = 2700 kg/m^3$. We discretize the bar using a uniform mesh of 40 two-node linear bar elements and compute the vibration

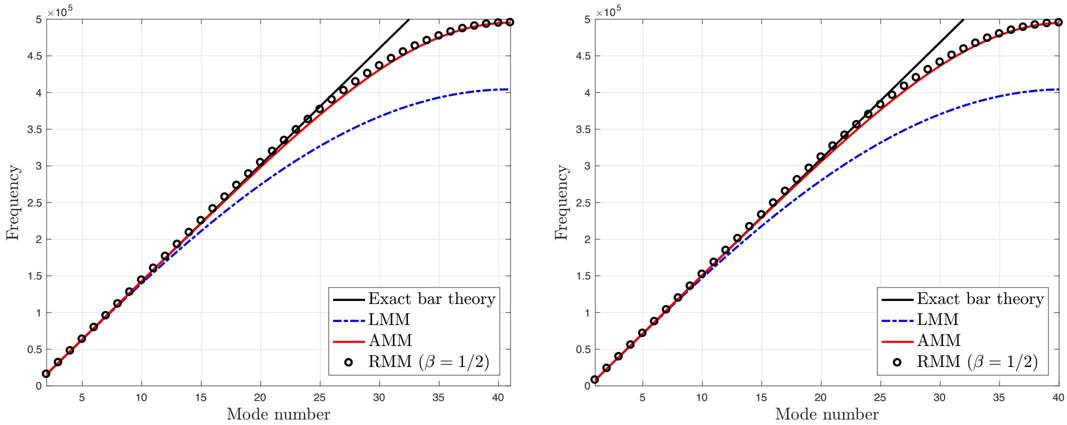

Figure 1: Bar vibration problem. Frequencies for the free-free (left) and fixed-free (right) cases. Comparison of exact frequencies and numerical frequencies obtained with: lumped mass-matrix (LMM), average mass-matrix (AMM) and the proposed inverse mass-matrix (RMM $\beta = 0.5$).

modes of the structure with different approximations for the mass-matrix inverse. In particular, we investigate differences in the use of the lumped mass-matrix LMM, averaged mass-matrix AMM and the proposed mass-matrix inverse computed through RMM with $\beta = 0.5$.

The results of the eigenvalue analysis are presented in Figure 1 for two different boundary conditions, free-free case (left) and fixed-free case (right). We start with the free-free case, by comparing the numerical frequencies with the exact solution obtained from continuum theory. The exact frequencies of this problem are $\omega_i^{exact} = \sqrt{E/L}(\pi/L)(i-1)$ rad/sec for mode number $i = 1, \dots n$ and the first eigenfrequency is zero, corresponding to the horizontal rigid body motion. We observe that the present method, utilizing the RMM, yields far better accuracy than the LMM and approximates very well to the AMM results for all frequencies.

For the fixed-free case, we obtain very similar results. The only difference now is in the restriction of the rigid body motion and the shift of exact frequencies to $\omega_i^{exact} = \sqrt{E/L}(\pi/L)(i-1/2)$ rad/sec for mode number $i = 1, \dots n$. We corroborate that the AMM and its approximation through the RMM with $\beta = 0.5$ provides exactly the same result. This means that the present method utilizing the inverse mass-matrix yields far better accuracy than the lumped mass-matrix with similar computational effort.

It can also be observed that LMM produces a maximum frequency around 20% lower than AMM, so the critical time-step for explicit time-integration can be reduced by the same amount using a diagonal mass-matrix. Even higher gains can be obtained with selective mass scaling techniques, maintaining at the same time the advantages in terms of accuracy of using a non-diagonal mass-matrix.

4.2 Frequencies of a free-free and a fixed-free beam

In this second case, we consider the same beam of the previous example but now it is discretized using 20 Euler-Bernoulli beam elements with two DOFs per node, i.e., deflection and rotation. We know that the shape functions for the Euler-Bernoulli beam require C^1-continuity for deflections and rotations, hence cubic Hermite polynomials are used as interpolation functions. This means that we would need to derive biorthogonal basis functions for the Hermite cubic shape functions in order to compute the reciprocal mass-matrix $\mathbf{C}_e$ from its definition (18). As previously described, we bypass this complex derivation obtaining the projection matrix $\mathbf{A}_e$ from the diagonalization of the element mass-matrix.

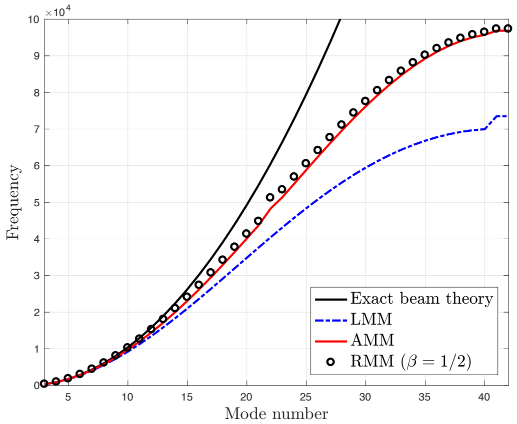

Figure 2: Beam vibration problem. Frequencies for the free-free (left) and fixed-free (right) cases. Comparison of exact frequencies and numerical frequencies obtained with: lumped mass-matrix (LMM), average mass-matrix (AMM) and the proposed inverse mass-matrix (RMM $\beta = 0.5$).

In Figure 2 (left) we analyze the frequencies obtained for the free-free beam case. The exact frequencies of this problem obtained from continuum theory are $\omega_i^{exact} = \sqrt{EI/\rho A}(c_i/L)^2$ rad/sec with $c = \{0, 0, 4.73, 7.853, 10.996, 14.137, 17.279, \dots\}$ for mode number $i = 1, \dots n$ and two zero frequencies corresponding to the displacement and rotation rigid-body motions. We solve again the problem with exact LMM and AMM inverse mass-matrices and then using the proposed RMM with $\beta = 0.5$. Results illustrate, first, that the consistent AMM gives far better accuracy than diagonal LMM for this particular case, specially in the high-frequency range. Secondly, that the present RMM method utilizing the inverse mass-matrix yields the same accuracy than the consistent AMM.

The results for the fixed-free alternative of this problem are represented in Figure 2 (right). The exact frequencies of this case are $\omega_i^{exact} = \sqrt{EI/\rho A}(c_i/L)^2$ rad/sec with $c = \{1.875, \dots\}$. Exactly the same precision is observed in the free-free and fixed-free solutions. This convinces us to the conclusion that the proposed method for generating the inverse of mass matrices M_b^{-1}, yields almost the same resonant frequencies as those obtained by the consistent mass matrices, as evidenced from Figure 2, thus confirming the validity of the present formulation.

5 CONCLUSIONS

A new methodology for direct generation of the inverse mass-matrix for discrete finite element equations of elastodynamics is presented, which is completely element-independent and does not require any special treatments of the elements adjacent to the Dirichlet boundaries. In the present method, the Dirichlet boundary conditions are handled by the method of localized Lagrange multipliers. This process is found to be computationally efficient, because matrices are sparse and only the factorization of a small matrix associated with the constrained DOFs is required.

The present inverse mass-matrices have been tested for rod and beam elements, demonstrating excellent accuracy in terms of frequencies and time evolution of the DOFs obtained with explicit time-integration methods.

REFERENCES

[1] Tkachuk A, Bischoff, M. Direct and sparse construction of consistent inverse mass matrices: general variational formulation and application to selective mass scaling. *Interna-*

tional Journal for Numerical Methods in Engineering 2015; 101:435-469.

[2] Park KC, Felippa CA. A variational framework for solution method developments in structural mechanics. *Journal of Applied Mechanics* 1998; **65**(1):242–249.

[3] Gonzalez JA, Park KC, Felippa CA, Abascal R. A formulation based on localized Lagrange multipliers for BEM-FEM coupling in contact problems *Computer Methods in Applied Mechanics and Engineering* 2007, Volume: 197 Issue: 6-8 Pages: 623-640.